Reconfiguration in Shipboard Power Systems

Kent Davey *Fellow*, *IEEE*, Raul Longoria*, *Member*, *IEEE,* William Shutt, Johnson Carroll, Keerthi Nagaraj, Jerad Park, Tom Rosenwinkel, Wei Wu, and , Ari Arapostathis*, Senior Member, IEEE*

***Abstract*—A shipboard power system is self contained, tightly coupled, and small enough to allow nearly real time state estimation, given the right equivalent circuit representations. Redirecting power flow is the preeminent task of reconfiguration. This redirection should be accomplished in less than two cycles, while never compromising system stability or power delivery to critical loads. These performance objectives can be approached using an equivalent impedance system representation and various optimization procedures. This reconfiguration control approach is demonstrated through a Matlab Simulink© simulation. Additional issues are addressed concerning the proper realization of a reconfigurable power system by incorporating gas turbine status, as well as due consideration for stable and safe transition between different power system states.**

I. Introduction

RECONFIGURATION is the restructuring of a system to achieve desired performance, resulting in a new system architecture. Power will flow from the primal source(s) to electrical loads through reconfigured paths. Some view reconfiguration as a tool to mitigate compromised conditions. However, if the speed of the reconfiguration algorithm and hardware is less than a few cycles, it offers the possibility of being a tool integral to the normal operation of a shipboard power system (SPS), guaranteeing optimal performance. It is viewed as imprudent to rely on a reconfiguration system integral to the survival of the ship under combat conditions that is exercised only under emergency conditions.

Two approaches to reconfiguration offer distinct yet possibly complementary ways to solve the SPS reconfiguration control problem. One approach is a bottom up line of attack, as might be taken with intelligent agents [1,2,3]. Agents may be designed to target a subset of the problem and are equipped with essential functionality, such as the ability to communicate with neighboring agents. They might, for example, ask if their control region has the ability to share some of its power with its neighbors.

The second approach is top down, in which decisions are based on global information gathered throughout the SPS. Control action at this level may be directly related to mission-specific needs and requirements, which must be reconciled with the monitored SPS state. This leads to decisions about reconfiguration. The basis for these decisions may focus on instantaneous power flow, for example, being derived from voltage and current flow data directly measured from key points in the system, which provide a measure of dynamic equivalent impedances [4]. Dynamic impedance measurement is considered a key element in SPS monitoring, as will be demonstrated in this paper.

This paper begins by describing how the second reconfiguration approach was adopted by this team, summarized as follows:

1. Based on the time data stream of current and voltage at every primary system node, determine the equivalent impedance configuration for the system.
2. Run an optimization algorithm, such as binary branch-and-bound, to determine the configuration that best uses the system resources, meets critical power demands, and minimizes losses.
3. Progress to the favored state through the most direct stable path, minimizing switching transients.
4. Repeat the process as soon as the switching transients have sufficiently decayed.

A simulation model has been developed and results for cases studies and its use for further evaluation of algorithm(s) are described. It becomes evident that certain sub-tasks are best handled by an intelligent agent, as only information about its immediate environment is needed to perform those tasks effectively. For example, voltage and current transients are generated when switching into a more favorable configuration. These can be minimized by ensuring switch closures at zero voltage crossings and switch openings at zero current crossings.

The paper also summarizes findings on how multiple gas turbine generators should be used in the most effective manner. In addition, modeling results are presented to guide optimal scheduling of generators, followed by insights into stability, particularly as it relates to making transitions between reconfigurable states. The integrated use of these results and the simulation modeling will support SPS reconfiguration and design tool development.

Manuscript received September 14, 2006. This work was supported in part by the Office of Naval Research.

Corresponding author, R. Longoria is with the University of Texas, Department of Mechanical Engineering, 1 University Station C2200, Austin, TX 78712 USA (phone 512-471-0530, fax 512-471-8727, email: r.longoria@mail.utexas.edu).

K. Davey is with the University of Texas, Center for Electromechanics, 1 University Station R7000, Austin, TX 78712 USA.

W. Shutt is with the University of Texas, Applied Research Laboratories, 1 University Station F0252, Austin, TX 78712 USA.

J. Carroll, K. Nagaraj, J. Park, T. Rosenwinkel, and W. Wu are students at the University of Texas, Austin, TX USA.

A. Arapostathis is with the University of Texas, Department of Electrical and Computer Engineering, 1 University Station C0803, Austin, TX 78712 USA.

II. Computing the Equivalent Impedances

The sampling of current and voltage in time periods much less than the fundamental period is not useful by itself. In a time harmonic system with primary frequency ω, these key parameters, such as current and voltage, can be represented over a short period of time with a magnitude and a phase. The ratio of the magnitudes and the difference of the phases is the key to rapid detection of faults. The current on two separate lines at time t and frequency ω can be written as

$$I_1 = \alpha \cos(\omega t) \tag{1}$$

$$I_2 = \beta \cos(\omega t - \phi) \tag{2}$$

One key to assessing system level status, including rapid fault detection, is the time history of the magnitude ratio α/β and the phase difference ϕ. Note that during a fault or system transient, the magnitude and phase will change. The magnitude itself can be expressed as a sinusoid or a sum of sinusoids with frequencies different from ω. The product of two sinusoids with different frequencies is equivalent to another sinusoid with a different frequency. Thus, this approach will handle the fact that the frequency is not really constant during a transient. The reader should note that dϕ/dt incorporates the change in frequency.

Suppose the currents are being sampled with Hall Effect probes at time interval δ*t*. Define the signals s_1 through s_6 as

$$\begin{aligned} s_1 &= A \cos(\omega t) \\ s_2 &= A \cos(\omega(t+\delta t)) \\ s_3 &= A \cos(\omega(t+2\delta t)) \\ s_4 &= B \cos(\omega t - \phi) \\ s_5 &= B \cos(\omega(t+\delta t) - \phi) \\ s_6 &= B \cos(\omega(t+2\delta t) - \phi) \end{aligned} \tag{3}$$

Observe that

$$\frac{A}{B} = \frac{s_1 \cos(\phi)\, s_2 \cos(\omega\, \delta t - \phi)}{s_4 + s_5 \cos(\omega\, \delta t)} \tag{4}$$

The assumption of phase 0 for signal s_1 is not a limitation since t is an arbitrary number. This expression is interesting, but not very useful unless the phase is known a priori. The problem is that the time is unknown and the sampling period is short. Consider rearranging this into three equations,

$$\begin{aligned} s_1 \cos(\omega t - \phi) &= \frac{A}{B} s_4 \cos(\omega t) \\ s_2 \cos(\omega(t+\delta t) - \phi) &= \frac{A}{B} s_5 (\cos(\omega(t+\delta t))) \\ s_3 \cos(\omega(t+2\delta t) - \phi) &= \frac{A}{B} s_6 (\cos(\omega(t+2\delta t))) \end{aligned} \tag{5}$$

These constitute three equations and three unknowns, time t, which is of no concern, the phase ϕ, and the magnitude ratio A/B. These equations have an extended analytic solution listed in [1], [2].

III. Grid Analysis

Once the equivalent impedances are known, one way to analyze a dynamic shipboard power system is to represent all components by their appropriate differential equations and continuously perform a transient system solution. An alternative to this unacceptably long procedure has been shown to be possible using equivalent series and parallel impedances to represent power transmission and useful load power, respectively. This representation is integral to the discussion that follows.

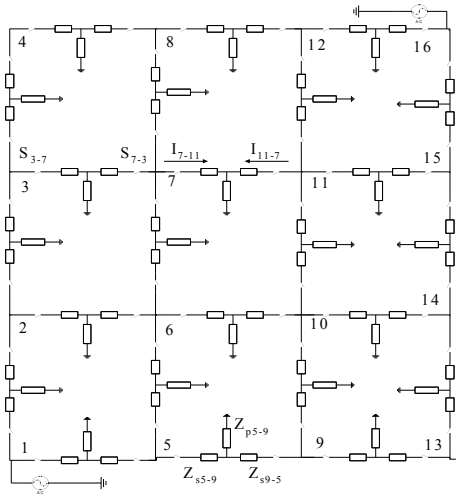

Fig. 1. Interconnected mesh grid represented with equivalent impedances.

The impedances in Fig. 1 are computed and updated in real time based on current and voltage measurements on a trunk line feeding each of the equivalent "T" loads. Reliable values of the impedance can be computed from an analytic equation and data from three consecutive measurements in about 1/5 of a cycle. Using this approach, the format of the grid equations becomes locked; only the values of the impedances change with time. State estimation code was written in C programming language and run on a 3 GHz Xeon processor to validate the speed of prediction. It was proven that the procedure could be performed in 2 microseconds per iteration.

A. The Optimization Problem

The objective during both steady state and compromised conditions is to maximize power delivery to all loads Z_p while minimizing transmission losses subject to the constraints that no line carries more than its rated current and that the power rating of the generators not be exceeded. Some loads are commonly more important than others. If a weighting index is assigned to the loads, the problem becomes one of minimizing the index

$$\begin{aligned} &\Im = \sum I_s^{\,2} R_s - \sum_{j=1}^{m} w_j I_{pj}^{\,2} Z_{pj} \\ &subj \\ &I_s \le I_{trunk\ Rating} \\ &Gen_{Load} \le P_{Rated} \end{aligned} \tag{6}$$

I_s is the series current, I_{pj} is the parallel load current in the

jth load, w_j is the weighting priority on the jth load, R_s is the series resistance, Z_{pj} is the parallel impedance of the jth load, $I_{trunk\ Rating}$ is the current limitation for the trunk lines show in Fig. 1, Gen_{Load} is the power delivered by the generator, and P_{rated} is the rated power for the generator.

IV. Simulation System Studies

Reconfiguration of a five-load shipboard power system (SPS) was studied by direct simulation for the purpose of evaluating key processes in the proposed algorithm illustrated in Fig. 2. The five-load system schematic shown in Fig. 3 is powered by two generators, and each load takes the form detailed in Fig. 4. The trunk lines that feed each load feature a controlled switch and the specification of these ten switch states is the task of a reconfiguration control scheme.

Three scenarios were chosen to test the responsiveness of the system monitoring approach using equivalent impedances. In addition, an algorithm was incorporated for transitioning from one reconfigurable state to another. Specifically, the individual switches were modeled with standard arc suppression logic (open when currents go to zero, close when voltage goes to zero), however it was desired to constrain the SPS system to transition in an acceptable manner. In these simulations, this meant requiring intermediate switch states to be introduced so that user-specified constraints are obeyed and system node equations are satisfied [7].

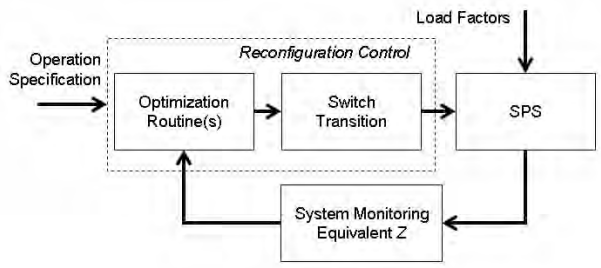

Fig. 2. Reconfiguration control diagram targeted by simulation study.

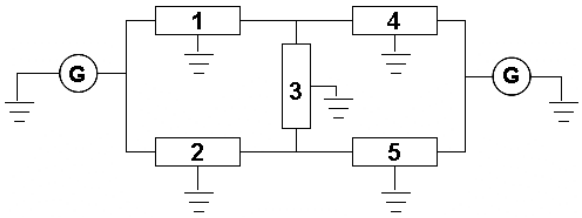

Fig. 3. Five-load system used for simulation studies.

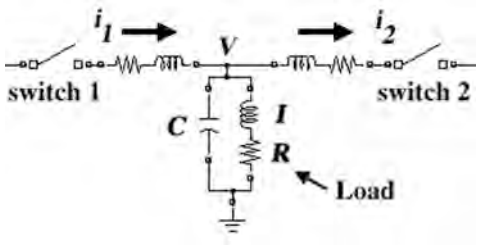

Fig. 4. Basic load circuit used in simulation model. Each load was fed by two trunk lines with controllable switches, 1 and 2, as shown.

The three scenarios include one defining 'nominal' operating conditions, where the goal is to maximize the objective function defined by equation (6). The other two scenarios are designed to test response to emergency situations: generator overload and line overload. In all of these situations, 'load factors' are used to simulate the need for reconfiguration. The load factors are signals that induce changes in the load system parameters.

The results were evaluated based on speed and accuracy. Speed, in this case, was defined as the time it takes to transition from one reconfiguration state to another. During a simulation, it is possible to monitor the actual switch state as well as the optimal switch state (specified by some optimization routine). This allows 'accuracy' to be defined by a metric distinguishing 'actual' and 'optimal'. In these studies, the focus was on the percentage of time that the actual switch configuration of the SPS was equal to 'optimal'. In these simulation studies, an exhaustive search algorithm was used in order to test accuracy. For practical implementation, other routines have been targeted for on-line application [8], [9].

A. Line Overload

To simulate a line overload, load 5 in Fig. 3 was given a step-wise reduction in load and the optimization routine was tasked with minimizing losses throughout the system while maintaining current specific current levels, especially in the trunk lines that feed load 5. A typical result is summarized in Fig. 5. The top graph in this figure shows the current in one of the trunk lines connected to load 5. The reconfiguration routine responds to the detected impedance change and reconfigures to an allowable state that does not induce an overload; the switch on the overloaded line is opened. This example is effective in illustrating how the equivalent impedance estimation can support a sub-cycle control effect.

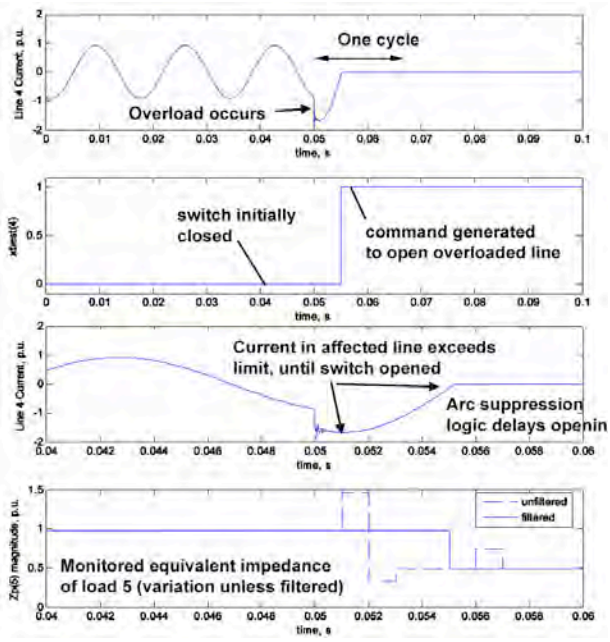

Fig. 5. Simulation of a line overload. The top graph shows current on a trunk line (detailed in third graph). The algorithm shows sub-cycle response time in opening the switch.

B. *Generator Overload*

The reconfiguration routine can also respond to conditions that will overload one of the generators. In this case, the simulation was used to study how well gradual changes in loads could be detected by the equivalent impedance technique. For this purpose, load 5 was allowed to gradually decay from an initial value. This required load 5 to be shed rather than overload the generators.

The simulation allowed study of load shedding algorithms, finding that it is necessary to transition the system through different reconfiguration states before finally shedding the load. It was also discovered in this study that gradual load changes are difficult to detect via equivalent impedance estimation, as compared to step changes (this is not uncommon in fault detection scenarios).

C. *Maximize Power Delivery and Minimize Losses*

It is highly desirable to have a reconfiguration control system that can optimize performance during *non-emergency situations*, as well as react to the type of fault conditions described earlier. To demonstrate such an ability, a scenario was simulated in which load 3 (Fig. 3) was increased, signaling a decreased power demand. Fig. 6 shows the initial configuration before this change occurs, where power demand is met with two open switches.

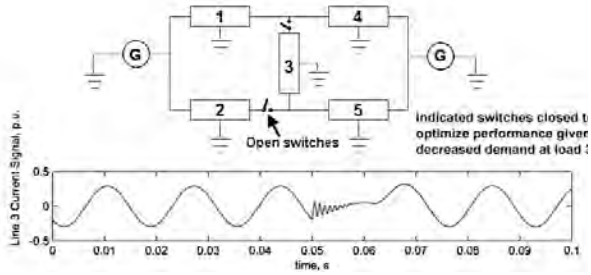

Fig. 6. The initial configuration is shown where optimal performance is achieved with the two open switches indicated. When load 3 demand decreases, it becomes necessary to close those switches, and this change is made within one cycle.

These three basic results reflect the type of simulation testing used to critically evaluate some of the key processes required for reconfiguration algorithms in SPS. Extended testing was conducted to determine some of the practical limitations of the equivalent impedance estimation method. The effect of noise and applied filtering/smoothing techniques are detailed in Park [7]. This work also describes the details of transition logic used in switching between two stable SPS states.

V. Extensions to Optimization of SPS

The baseline simulations on reconfiguration control presented in the previous section consider ideal generator models and utilized an exhaustive search routine to find optimal solutions. This section presents insight into how these simulations should be extended to reflect practical realities in the generator and the need for computationally-efficient optimization.

A. *The Complication of the Gas Turbine*

All new naval vessels are powered by gas turbines. If the gas turbine is added to the optimization, the objective is to minimize the fuel delivered to the gas turbine while still maximizing the useful power delivery throughout the grid. Previous work [3] made it clear that considerable fuel savings can be realized if multiple turbines of dissimilar size are used for primal power.

Specific fuel consumption of various commercial gas turbines as a function of power demand is shown in 7. The trend to note is that the larger systems exhibit higher fuel efficiency at higher power rating but much poorer efficiency at low power ratings than their smaller power counterparts. If the speed of the ship drops, and thus the power demand, it will always be more favorable to swap power from the larger turbines to the smaller as the power demand decreases.

How does this play out electrically? Suppose a high power load in Fig. 1 near nodes 12 or 14 is required. From an electrical perspective, drawing that power from the generator in the upper right hand corner would make the most sense. However, if the total power demand is low, and the upper hand corner turbine is large, then, switches should be thrown to redirect power flow from the lower generator. This consideration adds yet a deeper level of complexity to the reconfiguration optimization.

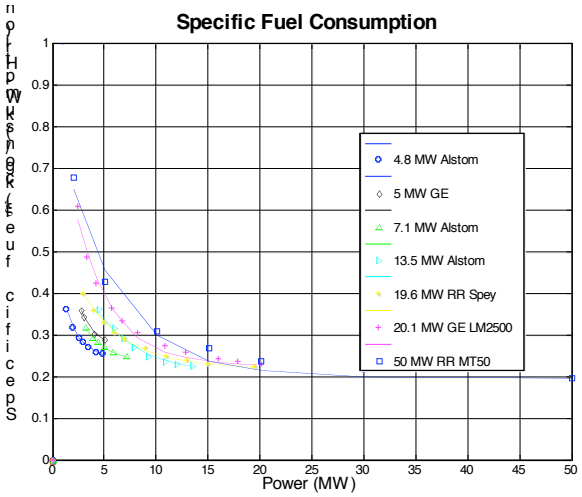

Fig. 7. Predicted versus measured specific fuel consumptions of various generators as a function of power demand.

B. *Optimization Extensions*

Binary-integer branch-and-bound algorithms have proven useful for solving (6). This approach and its results are discussed in [4]. Two stochastic methods have also been investigated for this type of problem [5]. In the latter work, a small test grid was employed to compare these methods with simplified loads, but with loads whose magnitudes relative to each other were representative of those found on a ship.

More recently Davey has shown that pattern search methods using Latin Hypercube local searches and appropriate penalty functions prove to be quite useful for this type of problem [6]. Although the stochastic methods such as genetic algorithm and simulated annealing are convenient, they also prove to be quite slow in comparison to the deterministic counterparts.

VI. Optimal Generator Scheduling

Consider the dynamic behavior of power generation and scheduling. With various energy storage technologies available, it is imperative to understand their impact on the dynamic power generation scheduling. Fig. 7 shows the specific fuel consumption for six commercial turbines. All turbines work most efficiently at peak load ratings, but lose considerable efficiency at partial power settings. Thus, intuitively, one should distribute the maximum load for some of the turbines and keep others idle. On the other hand, switching turbines from OFF to ON requires additional fuel for the start-up process. Therefore, there exists a tradeoff in balancing these two factors. Furthermore, by adding additional energy storage into the system, we can open up a new dimension for design and bring at least two advantages: first, it can reduce the frequency of turbines switching from OFF to ON, thus reducing their overhead; second, it can allow turbines to work mostly at peak load, the most efficient working point.

Consider formulating the dynamic generation scheduling of shipboard power systems as a controlled Markov process. We consider an electric ship with a number of N turbine-generators. The total power required for the ship at speed v_k is $\bar{P}_k$. Let $P_{n,k}$ denote the power assigned to Generator n at speed v_k.

The specific fuel consumption of Generator n denotes how much fuel is required to generate unit power at Generator n, and is typically an exponential function in $P_{n,k}$ (see Fig. 7).

Specifically,

$$\xi = \xi_0 + \frac{(\xi_2 - \xi_0)}{1 - e^{-m}} \cdot \left(1 - e^{-m\left(\frac{P - P_{\min}}{P_{\max} - P_{\min}}\right)} \right). \tag{7}$$

Given a mission profile, with η_k denoting the sojourn time fraction at speed v_k of a mission, generation scheduling can be formulated as the following optimization problem:

$$\min \sum_k \eta_k \sum_{n=1}^{N} P_{n,k} \xi_n(P_{n,k}) \tag{8}$$

$$\text{Subject to: } \sum_{n=1}^{N} P_{n,k} \geq \bar{P}_k \ . \tag{9}$$

However, the objective function in (8) is non-convex, thus the optimal solution is computationally hard to obtain. We use a convex approximation of (9) and obtain the approximate optimal solution using convex optimization.

However, the above formulation neglects the additional fuel consumption when generators switch from OFF to ON. We consider this effect by modeling the system as a Markov decision process.

(MDP), with state (k_t, n_{t-1}) and action $(n_t, P_{*,t})$, where n_t denotes the number of generators ON at time t, k_t denotes the state of the ship speed, and $P_{*,t}$ denotes the power vector $\{P_{i,t}, 1 \leq i \leq n_t\}$ at time t, $1 \leq k_t \leq K$, $1 \leq n_t \leq N$. Under the assumption that the speed of the ship changes according to an autonomous Markov chain, and denoting the startup fuel consumption for each generator c_{start}, the problem can be formulated as a MDP with state constraints:

Minimize

$$\limsup_{T \to \infty} \frac{1}{T} \sum_{t=1}^{T} \left[\sum_{n=1}^{N} P_{n,k} \xi_n(P_{n,k}) + (n_t - n_{t-1}) c_{start} \right] \tag{10}$$

$$\text{Subject to } \sum_{i=1}^{N} P_{i,t} \geq \bar{P}_{k_t}, \ \forall t \in N$$

Here we consider the infinite horizon long-term average cost and the optimal policy can be obtained by the value iteration algorithm. Details are omitted due to space limitations.

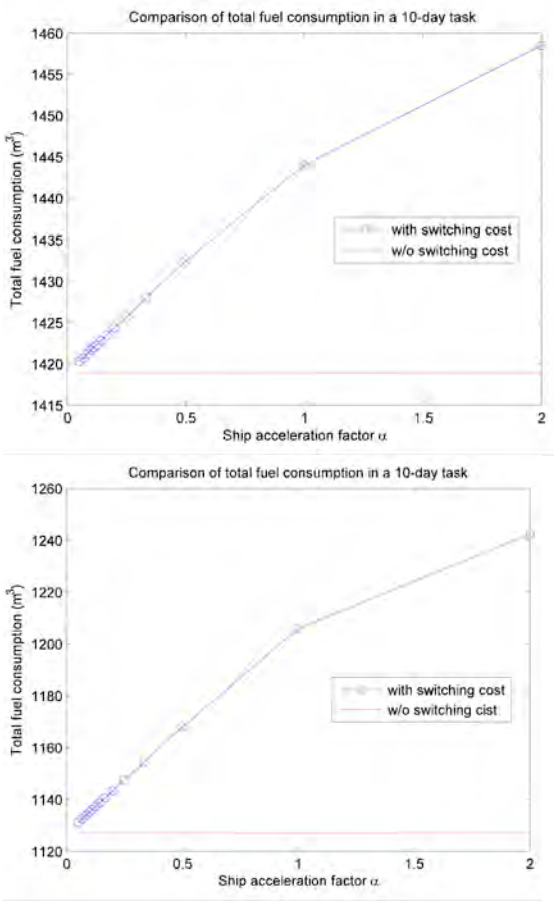

Fig. 8. Comparison of total fuel consumption between static optimization and dynamic optimization: (a) LM2500 turbine-generators; (b) Alstom turbine-generators.

In Fig. 8 we compare the total fuel consumption under the optimal power generation scheduling policy between the case without startup fuel consumption (i.e., c_{start}=0) and the case with startup fuel consumption. In Fig. 8(a), four LM2500 turbine-generators are used (N=4) and we consider a family of Markov chains characterizing the speed changes of the ship, which have the same stationary distribution (or mission profile) but different transition rates (acceleration factor of the ship). As we can see, with the transition rates increasing, the additional fuel consumption due to the startup fuel penalty also increases and can possibly be as much as 40 m^3 in certain cases. In Fig. 8(b), where six 13.5 MW Alston turbine-generators are used, the additional fuel consumption can be as much as 100 m^3, which is nearly 10% more than the expected fuel consumption obtained by the static optimization.

The results obtained suggest the following:

- It might be crucial to use power storage in electric ships to mitigate the impact of the startup fuel consumption and improve generation efficiency.
- We need to have control data of the ship acceleration distribution, and not only the mission profile, in order to be able to predict and accurately optimize the fuel consumption of generators.
- Adaptive optimal scheduling algorithms that tailor generation scheduling based on the most recent ship acceleration history might provide good solutions.

VII. Stability Issues

In order to analyze the safety and stability of a particular switching action, one must know something of the system trajectory beginning at the equilibrium of the first configuration and evolving under the dynamics of the target configuration. Rather than simulating the complete trajectory to test for safety and stability, one can use energy functions to estimate the region of the state space that will converge safely to the desired equilibrium. System theory results dictate that the energy of a dynamical system must decrease along trajectories. If a valid energy function exists, the safe region of convergence can be estimated by finding the largest energy value with a level set entirely contained within the safety bounds.

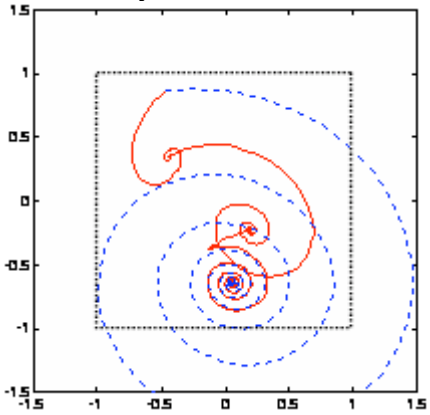

Fig. 9. Bounded energy level sets for 15 arbitrary 2-dimensional linear systems.

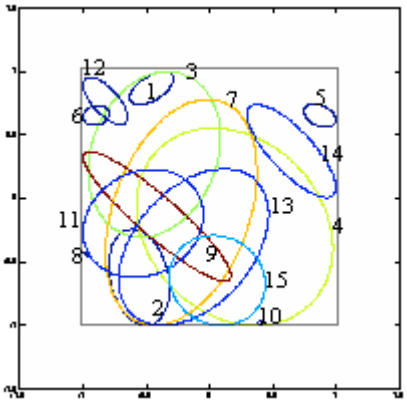

Fig.10. An unsafe transition (blue) and a safe switching path (red).

To illustrate the concept, Fig. 9 shows the critical energy level set for 15 arbitrary 2-dimensional linear systems bounded as shown. Fig. 10 shows how a multi-step switching path, chosen based on the level sets in Fig. 9, remains within bounds, while a direct transition does not.

VIII. Reconfiguration Optimization

A. Handling System Complexity

A great deal of work has been done over the years on developing energy functions for various power system models. However, most of the past work on energy functions for power system stability has focused on fault-based switching actions (i.e., breakers). However, in the reconfiguration problem we are interested in, every possible switching configuration is considered, not just the normal and faulted scenarios. Rather than working with the highly nonlinear dynamics of the system, we can linearize the singularly perturbed system model of each configuration around its respective equilibrium. Though the linearized version of the system is a rather extreme approximation, near the equilibrium it is reasonable and the analysis is greatly simplified.

Each switching configuration is represented generally by a differential-algebraic system,

$$\begin{aligned} \dot{x} &= f_Z(x,y) \\ 0 &= g_Z(x,y) \end{aligned}, \qquad (11)$$

which is then approximated as follows:

Singularly Perturbed System: $\begin{aligned} \dot{x} &= f_Z(x,y) \\ \varepsilon\dot{y} &= g_Z(x,y) \end{aligned}$; (12)

Linearized System: $\begin{bmatrix} \dot{x} \\ \dot{y} \end{bmatrix} = J_Z\left(\begin{bmatrix} x \\ y \end{bmatrix} - \begin{bmatrix} x_Z^{eq} \\ y_Z^{eq} \end{bmatrix}\right)$; (13)

Energy: $V\left(\begin{bmatrix} \dot{x} \\ \varepsilon\dot{y} \end{bmatrix}\right) = \left(\begin{bmatrix} x \\ y \end{bmatrix} - \begin{bmatrix} x_Z^{eq} \\ y_Z^{eq} \end{bmatrix}\right)^T P_Z\left(\begin{bmatrix} x \\ y \end{bmatrix} - \begin{bmatrix} x_Z^{eq} \\ y_Z^{eq} \end{bmatrix}\right)$, (14)

where P solves the Lyapunov equation for J.

B. Hard and Soft Constraints

For hard constraints, such as current limits, the quadratic energy function shown above allows the calculation of the critical energy level via quadratic optimization along each of the bounds on the state space. For constant loads and reference voltages, each of the optimizations may be performed off-line; if the loads and references will change, the linearized system can be maintained as a function of the continuous variables. A general cost function for optimization under soft constraints is expressed,

$$\sum_{n=1}^{N}\left(\underbrace{x_n^T P x_n}_{\substack{\text{Deviation from} \\ \text{the reference}}} + \underbrace{u_n^T Q u_n}_{\substack{\text{Cost on analog} \\ \text{control signal}}} + \underbrace{c(z_n)}_{\substack{\text{Switching} \\ \text{cost}}}\right) \qquad (15)$$

We also adopt a different approach by considering soft constraints: instead of restricting the voltages/currents to stay within a certain safe region, we optimize the hybrid trajectory so that the deviation from the reference voltages/currents is minimized. Furthermore, by adding a penalty on switching, within this framework, we reach a tradeoff of the optimality of the voltage deviation and the number of switches required. This model fits well into the framework of optimal control and stabilization of switching systems: the objective is to minimize the total accumulated cost of the deviation of the system state using analog controls and discrete controls which correspond to continuous feedback control and switching, respectively.

C. Reachability Graph

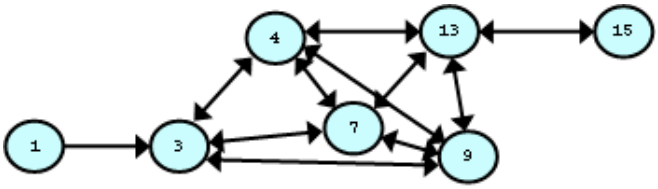


```
0 0 1 0 0 0 0 0 0 0 0 0 0 0
0 0 0 0 0 0 1 0 0 0 1 0 1 0 0
0 0 0 1 0 0 1 0 0 0 0 0 0 0 0
0 0 0 0 0 0 1 0 0 0 0 0 1 0 0
0 0 0 0 0 0 0 0 0 0 0 0 0 0 0
0 0 0 0 0 0 0 0 0 0 0 0 0 0 0
0 0 1 1 0 0 0 0 1 0 1 0 1 0 0
0 0 0 0 0 0 0 0 0 0 0 0 0 0 0
0 0 1 1 0 0 1 0 0 0 1 0 1 0 0
0 0 0 1 0 0 0 0 0 0 0 0 0 0 0
0 0 1 1 0 0 1 0 1 0 0 0 1 0 0
0 0 0 0 0 0 0 0 0 0 0 0 0 0 0
0 0 0 1 0 0 1 0 1 0 0 0 0 0 1
0 0 0 0 0 0 0 0 0 0 0 0 0 0 0
0 0 0 1 0 0 1 0 0 0 0 0 1 0 0
```

Fig.11. A partial reachability graph (above) and the complete reachability matrix (below) for the linear systems used in previous figures.

After the above analysis has been performed exhaustively on valid switching configurations, the resulting transition information can be formed into a reachability graph as follows. Each configuration is represented by a node, and each safe transition is indicated by a directed edge between nodes. As an illustrative example, Fig. 11 shows a partial reachability graph based on the 2-dimensional linear systems used in the previous figures. Because the graphical representation quickly becomes overcrowded, the reachability graph is also conveniently shown in matrix form (see Fig. 11). A 1 in the (i, j)th position indicates a safe transition from configuration i to configuration j.

IX. Conclusion

A top down reconfiguration strategy has been presented wherein the state of the electrical system is approximated using equivalent impedances computed dynamically with real time voltage and current measurements. Examples involving generator and line current overload were discussed and presented. These simulations suggest that the shortest reconfiguration time may be about one cycle. Shorter times encounter inaccurate equivalent impedances adversely influenced by switching transients. Future work in this area should be given to the gas turbine efficiency and its part in choosing optimal switching states.

References

[1] K. R. Davey and R. E. Hebner, "A new strategy for representation and control of self-contained power systems," *IEEE Trans. on Power Delivery*, vol. 21, no. 3, pp. 1558-1564, July 2006.
[2] K. Davey, "Fault analysis on a naval power grid using equivalent impedances," *IASME Trans.*, vol. 1, no. 2, pp. 247-252, April 2004.
[3] K. Davey, "Ship component in hull optimization," *Marine Technology Society Journal*, vol. 39, no. 2, pp. 35-42, 2005.
[4] K. Davey and R. Hebner, "Reconfiguration of shipboard power systems," *IASME Trans.*, vol. 1, no. 2, pp. 241-246, April 2004.
[5] C. D. Meek, "Investigation of optimization methods used for reconfiguration of the naval electric ship power system," M.S. Thesis, University of Texas, 2004.
[6] K. Davey, "Latin hypercube sampling and optimization in an electric ship," Electric Ship Research and Development Consortium August Meeting, Lafayette, Indiana, August 17-18, 2006.
[7] J. A. Park, "Dynamic modeling and analysis of an automatic reconfigurable shipboard power system," M.S. Thesis, University of Texas at Austin, 2006.
[8] C. Rehtanz, *Autonomous systems and intelligent agents in power system control and operation*, Springer, Berlin, 2003.
[9] K.L. Butler-Purry, "Multi-agent technology for self-healing shipboard power systems," *Proceedings of the 13th International Conference on Intelligent Systems Application to Power Systems*, November 6-10, 2005, pp. 207-211.
[10] K. Huang, D.A. Cartes, and S.K. Srivastava, "A multi-agent based algorithm for mesh-structured shipboard power system reconfiguration," *Proceedings of the 13th International Conference on Intelligent Systems Application to Power Systems*, November 6-10, 2005, pp. 188-193.